



Heterogeneous & Homogeneous & Bio- & Nano-

# CHEM **CAT** CHEM

---

## CATALYSIS

### Accepted Article

**Title:** Synthesis of textured tungsten disulfide nanosheets and their catalysis for benzylamine coupling reaction

**Authors:** Hua Liang, Bingqian Zhang, and Ji-Ming Song

This manuscript has been accepted after peer review and appears as an Accepted Article online prior to editing, proofing, and formal publication of the final Version of Record (VoR). This work is currently citable by using the Digital Object Identifier (DOI) given below. The VoR will be published online in Early View as soon as possible and may be different to this Accepted Article as a result of editing. Readers should obtain the VoR from the journal website shown below when it is published to ensure accuracy of information. The authors are responsible for the content of this Accepted Article.

**To be cited as:** *ChemCatChem* 10.1002/cctc.201901576

**Link to VoR:** <http://dx.doi.org/10.1002/cctc.201901576>

WILEY-VCH

[www.chemcatchem.org](http://www.chemcatchem.org)



**Synthesis of textured tungsten disulfide nanosheets and their  
catalysis for benzylamine coupling reaction**

Hua Liang<sup>§</sup>, Bing-Qian Zhang<sup>§</sup>, Ji-Ming Song\*

School of Chemistry & Chemical Engineering,

Anhui Province Key Laboratory of Chemistry for Inorganic/Organic Hybrid

Functionalized Materials,

Anhui University,

Hefei, Anhui 230601, P R China.

Tel: +86 0551 63861279 : Fax: +86 0551 63861279

*E-mail: jiming@ahu.edu.cn*

§These authors contributed equally to this article.

Accepted Manuscript

**Abstract:** Tungsten disulfide ( $\text{WS}_2$ ) has a graphite-like structure with the properties of strippable and indirect/direct band gap conversion, which makes it have important applications in the fields of optoelectronics, catalysis and lubrication. Here, ultra-thin  $\text{WS}_2$  nanosheets with texture on the surface were obtained by colloid synthesis method, and its phase, morphology and valence state were characterized. TEM images displayed that the obtained sample had flower-like morphology composed of “petal” nanosheets with several stripes on the surface. Interestingly, the fabricated  $\text{WS}_2$  nanosheets exhibited excellent catalytic performance for the conversion of benzylamine with the yield reaching 97.9% and excellent catalytic activity still being retained after 5 cycles of catalysis, and the  $\text{WS}_2$  nanosheets also had good catalytic activity for coupling reactions of benzylamine homologues to synthesize corresponding imines. Besides, the coupling reaction could be done in natural light without the need for additional light and oxygen atmosphere at certain temperature. Further research showed that in our reaction system, the benzylamine oxidative coupling reaction was a photothermal co-catalytic process with thermal catalysis being dominant role and photocatalysis further improving the yield.

## Introduction

Transition metal chalcogenides include a big family with the characteristics of layered structure and tunable band gaps, which exhibit good electric and optical properties.<sup>[1-3]</sup> As a member of the big family, tungsten disulfide (WS<sub>2</sub>) nanosheet has recently attracted widespread attention from scientists by virtue of its good photoluminescence effect<sup>[4-6]</sup> and considerable absorption intensity in the visible range as well as excellent mechanical properties and flexibility.<sup>[7]</sup> There are many synthesis methods to be developed to prepare WS<sub>2</sub> nanosheets, including stripping,<sup>[8]</sup> vapor deposition,<sup>[9]</sup> solvothermal<sup>[10]</sup> and colloidal method.<sup>[11]</sup> The colloidal synthesis has the advantages of simple and fast synthesis method with large amount and controllable morphology of products, which is favored. The geometric crystallization indicates that the monolayer tungsten disulfide displays a sandwich-like structure composed of three layers of atoms, where the sulfur atoms are located on the outer layer, and the tungsten atom is located on the inner layer. Because of its unique crystal structure, it has excellent optical and electrical properties.<sup>[5]</sup> So, the application of WS<sub>2</sub> nanosheets in the field of catalysis is worth exploring.<sup>[12-14]</sup>

The imine, as key intermediate in many reactions, has wide applications in the fields of industry, agriculture and biological medicine.<sup>[15-16]</sup> It can not only be used to synthesize corresponding nitrogen-containing organic compounds, drugs, biochemical active substances and natural products, but also possess unique bacteriostatic, bactericidal, antitumor, antiviral biological activities and good coordination chemical properties. Imines could be obtained by several synthesis methods, such as hydrogenation coupling reaction of nitro compounds,<sup>[17-18]</sup> oxidative condensation of

amines with alcohols.<sup>[19-20]</sup> Oxidative Coupling Reaction of Benzylamine (OCRB) is one of the effective ways to prepare corresponding imines. Mou prepared N-benzylidene benzylamine via OCRB under visible-light irradiation using Au/TiO<sub>2</sub> as catalyst.<sup>21</sup> In addition, precious metals and their alloys, such as Pd<sub>3</sub>Pb,<sup>[22]</sup> Au,<sup>[23-24]</sup> Au-Pd nanoparticles,<sup>[25]</sup> were also used as catalysts to prepare imines via OCRB. However, these reactions often require precious metals as catalysts with complex synthesis steps and harsh reaction conditions, which limit the development of these synthetic methods. So, researchers have been looking for cheap and efficient catalysts for coupling reaction of benzylamine.<sup>[26-28]</sup> However, to our best knowledge, the application of WS<sub>2</sub> in catalytic coupling reaction of amine has been rarely studied and its photothermal co-catalysis has not been reported.

In this work, we successfully synthesized the petal-like WS<sub>2</sub> nanosheets with 2H phase by oil phase method. The obtained WS<sub>2</sub> nanosheets were used as catalyst for coupling reaction of benzylamine, and we found that the conversion of benzylamine to imine was more than 97% under the conditions of 60 °C, air atmosphere, and natural light. Different reaction conditions, including different solvents, temperature, reaction time were explored. Interestingly, the oxidative coupling reaction of benzylamine in our reaction system was a photothermal co-catalytic reaction, and thermal catalysis played a leading role. The catalysts had good reaction activity and cycle stability after undergoing five cycles. Furthermore, it also had excellent catalytic activity for the benzylamine homologs.

## Experimental section

## Chemicals and characterization (see the Supporting Information, SI)

### Synthesis of WS<sub>2</sub> nanosheets

Preparation of precursor solution: 0.5 mmol tungsten hexachloride (WCl<sub>6</sub>) was dissolved in 2 ml oleic acid (OA) for 10 min by ultrasound until the color of the solution turned brown; then 20 ml of oleylamine (OLA) was added with magnetic stirring, and yellow solution was formed; 1 mmol sulfur powder was added to the above yellow solution and the orange **precursor solution** was obtained under magnetic stirring.

Next, 40 ml OLA was placed in a 100 ml three-neck flask and degassed at 65°C for 1 hour to remove the low-boiling substance, then was heated up to 320°C with nitrogen condition; the above **precursor solution** was slowly injected into the three-neck flask, and the mixed solution was kept at 320°C for one hour, then naturally cooled to room temperature. The final product was obtained by centrifugation and washing using a mixture of ethanol and chloroform for several times, then dried in a vacuum oven for later characterization and testing.

### Catalytic and cycle experiments of benzylamine coupling reaction

In the typical catalytic process, 0.5 mmol benzylamine as substrate, 30 mg WS<sub>2</sub> as catalyst and 0.5 ml acetonitrile as solvent were added in the Schlenk tube. The reaction mixture was heated to 60°C in an oil bath with magnetic stirring for 30 h. After the reaction, the catalyst was separated by centrifugation, and the supernatant was taken and determined by gas chromatography (GC) and gas chromatography-mass spectrometry (GC-MS). The effect of different solvents, such as n-hexane, ethanol and water, on the yield of the reaction was explored, and

acetonitrile was replaced by certain solvent in catalytic process, while other conditions remained unchanged. In addition, reaction temperature and catalyzed coupling of benzylamine homologues experiments with single conditional change was also investigated, and other experimental conditions were the same as typical experimental conditions.

### Recycle experiments of WS<sub>2</sub> as catalyst

The recycle stability of benzylamine coupling catalyzed by WS<sub>2</sub> nanosheets was explored, and five cycle experiments were carried out. The catalyst was separated by centrifugation after each reaction, and the supernatant was taken and determined by GC, then trichloromethane was used as dispersing agent and ethanol was used as precipitator for washing the catalyst for several times under the aid of centrifugation, and the regenerated catalyst was dried in a vacuum drying box at 60 °C for the next reaction.

## Results and Discussion

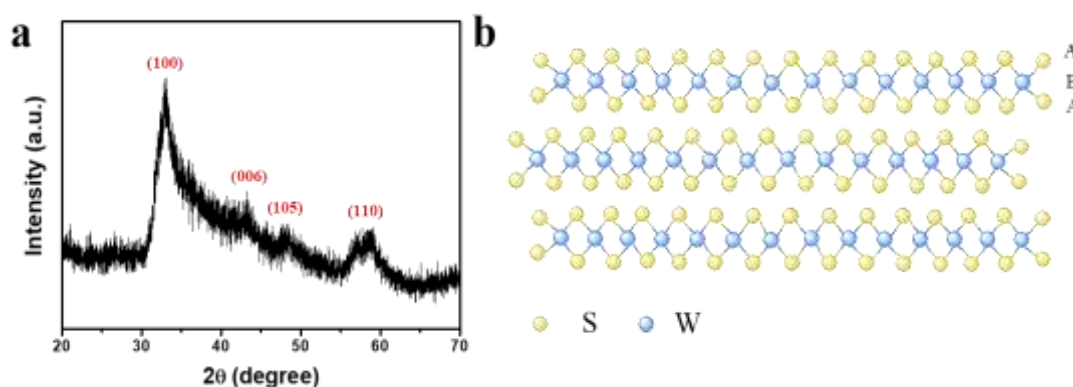


**Figure 1** (a) XRD pattern of the obtained samples, (b) The schematic diagram of WS<sub>2</sub> crystal structure

The phase analysis of the synthesized product was measured by XRD. As shown in Figure 1a, the product was the WS<sub>2</sub> of 2H phase.<sup>[11]</sup> There was a strong diffraction peak around 34° corresponding to the (100) crystal plane of WS<sub>2</sub>, while other

diffraction peaks at  $42^\circ$ ,  $48^\circ$  and  $58^\circ$  arose from the (006), (105) and (110) crystal planes, respectively. The apparent asymmetry of the diffraction peak corresponding to the (100) in the XRD pattern might be caused by the superposition of the diffraction peaks of the oxides on the surface of the sample, which could be learned from the subsequent XPS characterization. Figure 1b was the schematic diagram of 2H-WS<sub>2</sub> crystal structure, in which sandwich structure was composed of three atomic layers from the diagram by hexagonal closest stacking.<sup>[29]</sup> The layered WS<sub>2</sub> was formed by the combination of single-layer structure with van der Waals forces.

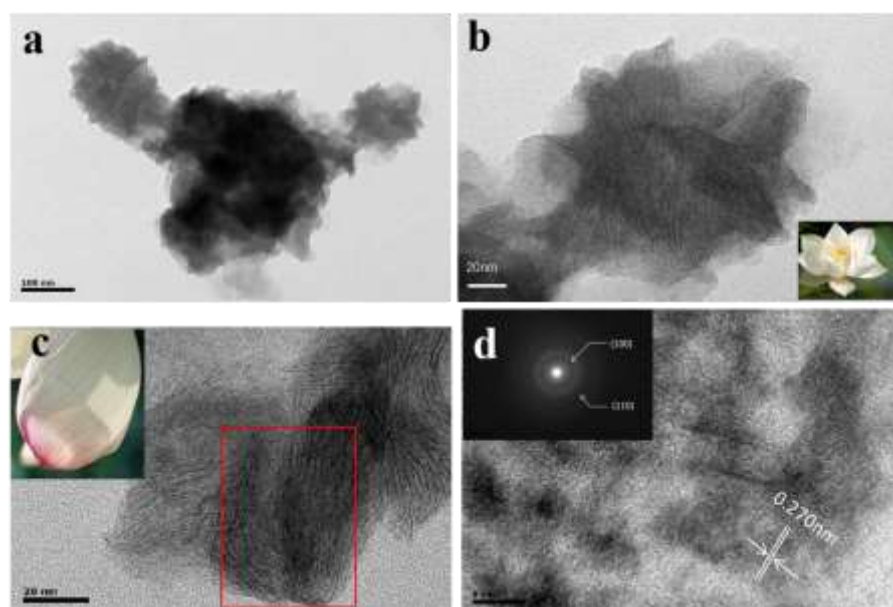


**Figure 2** (a), (b), (c) TEM images of the obtained samples and the illustration in Figure 2 (b, c) were photographs of a lotus and single petal with veins, respectively, (d) HRTEM image of the obtained sample, and the inset showed the SAED pattern.

Figure 2 showed the morphology and structure of the obtained WS<sub>2</sub> at different magnification. Figure 2a and Figure 2b revealed that the WS<sub>2</sub> displayed a flower-like morphology, which was similar with a lotus (inset in Figure 2b). From the local magnification diagram of Figure 2c, we could find that the single “lotus” was composed of many petals with several stripes on the surface of the petal (inset in

Figure 2c). HRTEM images showed the lattice-stripe distance was 0.270 nm corresponding to the (100) crystal plane of WS<sub>2</sub>, and the SAED pattern displayed two distinct diffraction rings correspond to (100), (110) crystal planes in Figure 2d, respectively.

Figure 3 displayed the XPS spectra of 2H-WS<sub>2</sub>. It could be observed from Figure 3a that the two characteristic peaks near 31.8 eV and 34.0 eV were attributed to W4f<sub>7/2</sub> and W4f<sub>5/2</sub>, respectively; the two peaks at 33.3 eV and 35.3 eV were derived from W 4f<sub>7/2</sub> and W4f<sub>5/2</sub> of W-O bond due to surface oxidation of the sample;<sup>[30-31]</sup> the wide peak at 37.6 eV was belong to XPS spectrum of W5p. Figure 3b showed that the XPS spectra of S 2p<sub>3/2</sub> and S 2p<sub>1/2</sub>, and the two characteristic peaks were located at 161.5 eV and 162.8 eV,<sup>[32-33]</sup> respectively.

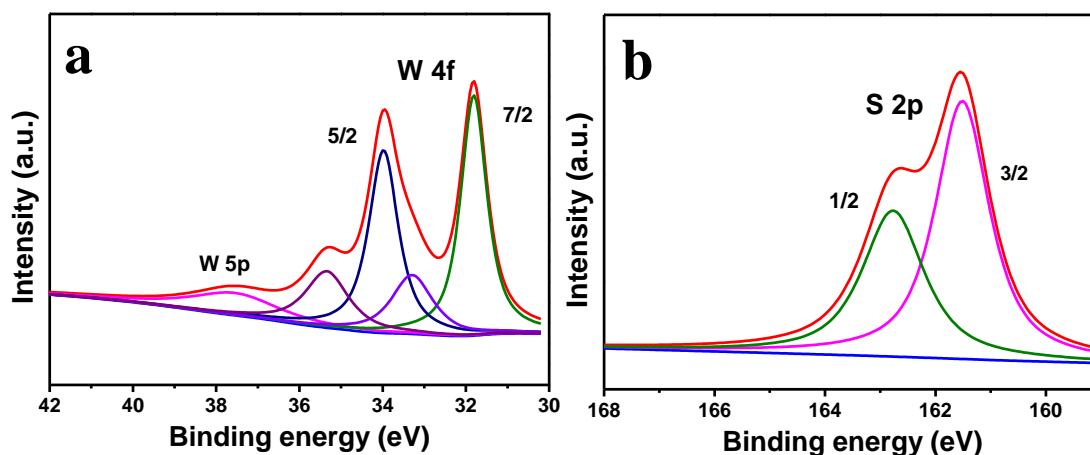


**Figure 3** XPS spectra of the WS<sub>2</sub>: (a) W 4f and (b) S 2p

The UV-Vis, Fluorescence, and Raman spectra of the obtained WS<sub>2</sub> nanosheets were shown in the Figure 4. There was an obvious broad absorption band in the range of 200-800 nm, indicating the WS<sub>2</sub> had good light absorption capacity, which would be beneficial to photocatalysis (Figure 4a). According to Tauc

formula  $(\alpha h\nu)^2 = C'(h\nu - E_g)$ , the extrapolated band gap of WS<sub>2</sub> was about 1.5 eV (Figure 4b), which was consistent with the band gap of the single-layer WS<sub>2</sub> nanosheets reported in the literature.<sup>[34]</sup> Figure 4c showed photoluminescence spectrum of WS<sub>2</sub> nanosheets, and the maximum emission wavelength was 405 nm using 260 nm as the excitation light with broadening peak shape. Figure 4d displayed that Raman spectra of the product, and two peaks at 350, 417 cm<sup>-1</sup> could be assigned to E<sub>2g</sub> mode and A<sub>1g</sub> mode of 2H-WS<sub>2</sub> nanosheets, respectively; this result indicated that the synthesized WS<sub>2</sub> nanosheet had a structure with individual and few layers.<sup>[35]</sup>

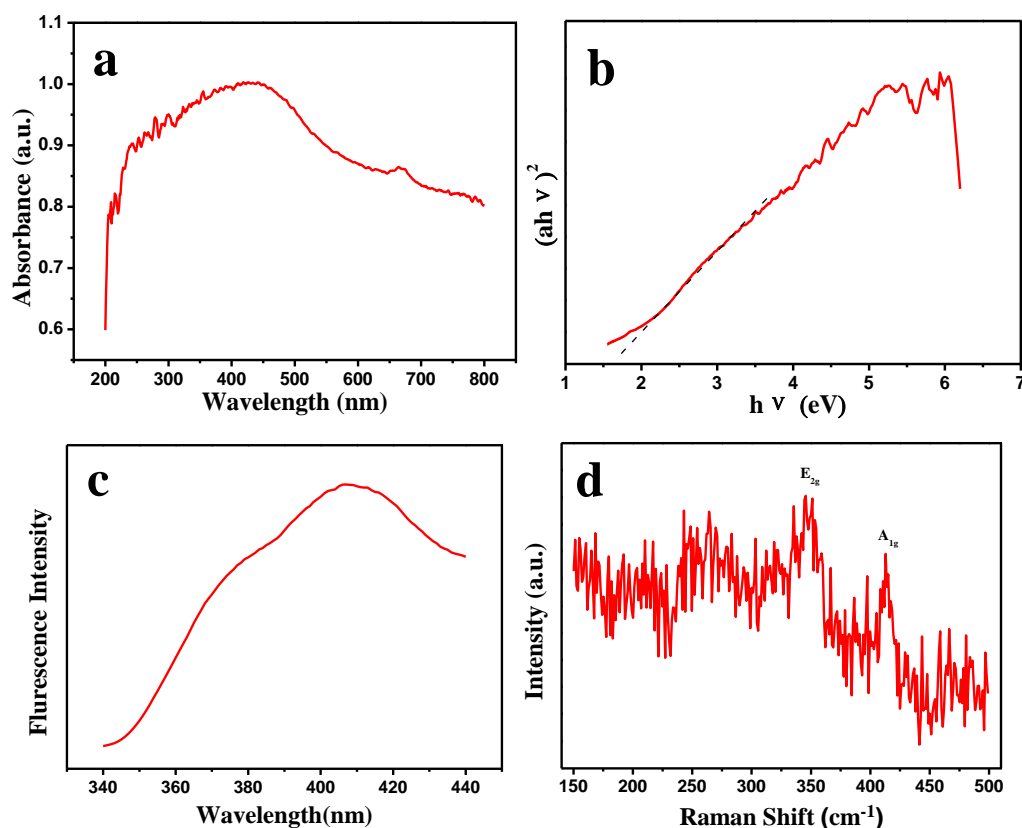


**Figure 4** Several spectra of WS<sub>2</sub>: (a) UV-Vis, (b) Tauc plot of UV-Vis, (c) Fluorescence, (d) Raman.

Then, the catalytic performance of the obtained WS<sub>2</sub> nanosheets was examined by using benzylamine being oxidized to imine as the probe reaction. The steps of the catalytic coupling reaction were referred to in the experimental section. Some reaction

conditions, such as reaction temperature, the effect of catalyst and solvents, have been explored (See SI, Figure S1, Table S1). We found that if there were no catalysts (WS<sub>2</sub> nanosheets) being added into the reaction system, the other experimental conditions were consistent with typical synthesis conditions and no coupling product N-benzylidene benzylamine was detected, indicating that WS<sub>2</sub> nanosheets played a crucial role in the coupling reaction of benzylamine. From the results of different temperatures, we found that the optimum temperature was 60 °C. Then, the catalytic reactions in different solvents such as acetonitrile, n-hexane, cyclohexane, ethanol and aqueous were carried out (Table 1 Entry 1-5). The results could be seen from Table 1, when acetonitrile was used as the solvent, the yield, conversion, and selectivity reached as high as 97.9%, 98.6% and 99.3%, respectively, after 30 hours of reaction. This yield was higher than the reported value (94%) in the literature with catalytic conditions of oxygen atmosphere and 5 W LED light source for 30 h.<sup>[36]</sup> When n-hexane or cyclohexane was used as solvents, the yields were 76.1% and 70.0% in turn, as well as favorable conversion and selectivity (Table 1 Entry 2-3).

**Table 1.** Oxidative coupling of benzylamine catalyzed by WS<sub>2</sub> nanosheets.

Entry	WS <sub>2</sub>	Conv. (%)	Sel. (%)	Yield (%)
1	acetonitrile	98.61	99.29	97.91
2	n-hexane	94.27	80.72	76.09
3	cyclohexane	78.69	88.97	70.01
4	ethanol	41.46	98.79	40.96
5	water	65.69	52.33	34.38

Reaction conditions: 0.5 mmol of benzylamine, 30 mg catalyst, air, 60°C for 30 h, determined by GC.

However, if the catalytic reactions were carried out in ethanol or water as solvents, the yields were only 41.0% in ethanol and 34.4% in water, respectively (Table 1 Entry 4-5). Therefore, like typical synthesis conditions, we chose the obtained WS<sub>2</sub> nanosheets as the catalyst and acetonitrile as a solvent to conduct experiments at 60 °C under natural light. Natural light in the laboratory could meet the experimental lighting requirements, without the use of sunlight or LED additional light sources. Reaction kinetic experiments showed that the catalytic coupling reaction of benzylamine in acetonitrile belonged to the first order reaction (Figure S3).

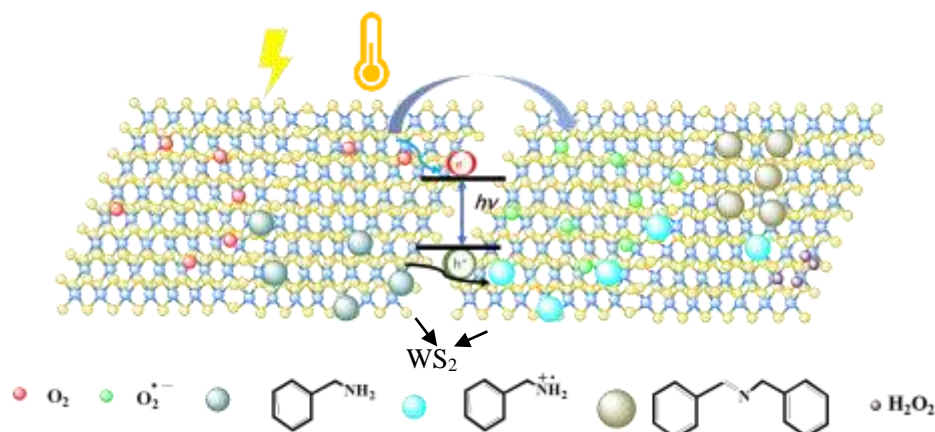
In order to determine the role of light and heat in the catalytic process, we further investigated the effects of temperature and light on the catalytic reaction. The reaction in the dark chamber for 30 h was carried out and kept the other conditions unchanged; the result displayed that the yield obtained was 93.2%, slightly lower than the yield (97.9%) under typical catalytic condition. Therefore, the benzylamine coupling reaction could be well carried out in the dark chamber for our catalytic reaction system. To further prove the relationship between photocatalysis and thermocatalysis, we carried out the experiments under natural light and dark at 20 °C and 60 °C for 12 h, respectively. The results showed that the yield of reaction under darkroom at 20 °C was 10.5%, while the yield in darkroom at 60 °C was 63.2%, which yield could be further increased to 80.4% when natural light was introduced at the same time. As a comparison, when there was only natural light without heating (room temperature), the yield was only 12.9% as shown in Table 2. Therefore, we can conclude that the

oxidative coupling reaction of benzylamine in our reaction system was a photothermal co-catalytic reaction, and thermal catalysis played a leading role.

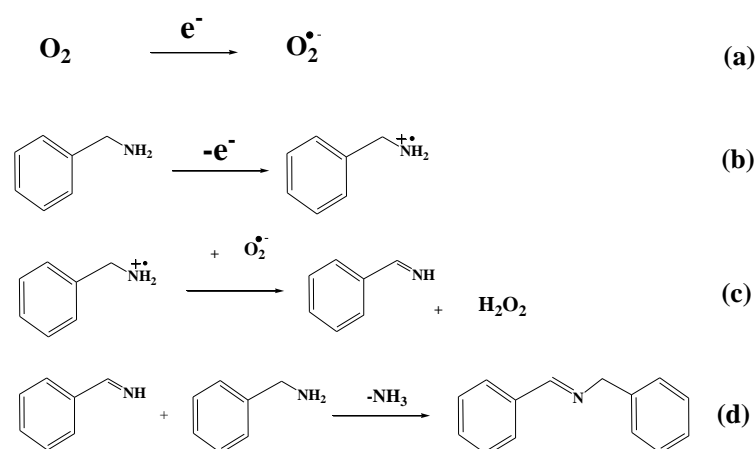
**Table 2.** Catalytic Performances of WS<sub>2</sub> under different conditions

Entry	T (°C)/ Light	Time (h)	Yield (%)
1	60 / natural light	30	97.9
2	60 / dark	30	93.2
3	60 / natural light	12	80.4
4	60 / dark	12	63.2
5	20 / natural light	12	12.9
6	20 / dark	12	10.5
7	60 /blue light	12	77.8
8	60 /red light	12	72.1
9	60 /fluorescent lamp	12	68.8

In addition, the effect of different light sources, such as blue light, red light, and fluorescent lamp, on the catalytic reaction were also investigated at 60 °C for 12 h. As shown in Table 2, under the irradiation of blue and red light source, the yield of the reaction at 60 °C for 12 h was 77.8% and 72.1%, respectively. The yield was 68.8% when irradiation under fluorescent lamp with 60 W in laboratory. Those results showed that different light sources had certain effects on the catalytic yield with little difference, which were consistent with the fact that the reaction was dominated by thermal catalysis, and the catalyst WS<sub>2</sub> had good absorption in a wide wavelength range (Figure 4a).

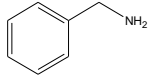
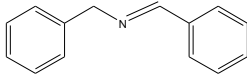
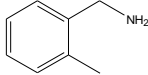
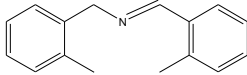
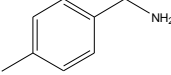
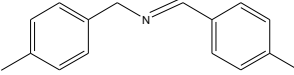
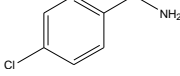
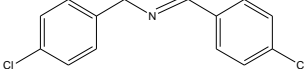
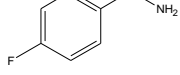
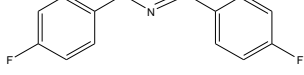


**Figure 5** Schematic diagram of proposed mechanism for the oxidative coupling of benzylamine catalyzed by WS<sub>2</sub> nanosheets



The mechanism of the catalytic reaction process was illustrated in Figure 5 and Formula (a-d). Firstly, under the irradiation of hot source and natural light, electron-hole pairs were generated on the surface of the WS<sub>2</sub> nanosheets, and large quantities of electron were captured by the adsorbed oxygen to produce superoxide radicals with very high reaction activity; meanwhile, benzylamine captured the positive charge from the hole and formed benzylamine radicals (Formula a and b). Secondly, freshly formed benzylamine radicals further reacted with superoxide radicals to form hydrogen peroxide and corresponding benzamide (Formula c). Finally, reaction between benzamide and benzylamine produced the final product by deamination (Formula d).<sup>[37]</sup>

**Table 3.** Oxidative coupling reaction of several benzylamine homologues catalyzed by WS<sub>2</sub> nanosheets.

Entry	Reactants	Products	Yield (%)
1			97.91
2			92.80
3			93.97
4			94.93
5			96.19

Reaction conditions: 0.5 mmol benzylamine or its homologue, 30 mg WS<sub>2</sub>, Air, 60°C, 30 h, determined by GC-MS.

To demonstrate the formation of superoxide radicals during the reaction, we used p-benzoquinone as superoxide radical scavenger to verify. At the beginning of the reaction, an appropriate amount of p-benzoquinone was added to the reaction system, and other conditions remained unchanged. The catalytic results showed that the yield was only 0.94% (Table S2, 2<sup>a</sup>), indicating that most of the superoxide radicals generated during the reaction were captured by p-benzoquinone, which greatly reduced the reaction rate. Besides, a DPD/POD method was used to detect the content of hydrogen peroxide in the reaction process. The results revealed that two peaks of the hydrogen peroxide signal appeared near 510 nm and 551 nm (Figure S2), indicating that the superoxide free radicals reacted with benzylamine radicals to produce hydrogen peroxide (Formula c).<sup>[38]</sup>

Based on those results, oxidative coupling of a series of benzylamine homologues using  $WS_2$  as catalyst was tested. The results could be seen from Table 3 that  $WS_2$  nanosheets had same great catalytic performance for the coupling reaction of a variety of benzylamine homologues, and all yields were higher than 92% (Table 3 Entry 2-5). Furthermore, we could see that those yields were slightly lower than that of benzylamine (Table 3 Entry 1), which might be related to the type and position of substituent group on the benzene ring. The methyl group belongs to the electron donor group, when it is in the ortho-position and para-position of the benzylamino group, the electron cloud density of the benzene ring increases, thereby increasing the p- $\pi$  conjugate effect and reducing the reaction activity of the benzylamine homologue. While the halogen atom is an electron-absorbing group, which can reduce the density of electron cloud, thereby reducing the p- $\pi$  conjugate effect with the amine group and increasing the amino group reaction activity, and the greater the halogen polarity, the more obvious the effect (Table 3 Entry 2-5).<sup>[39]</sup>

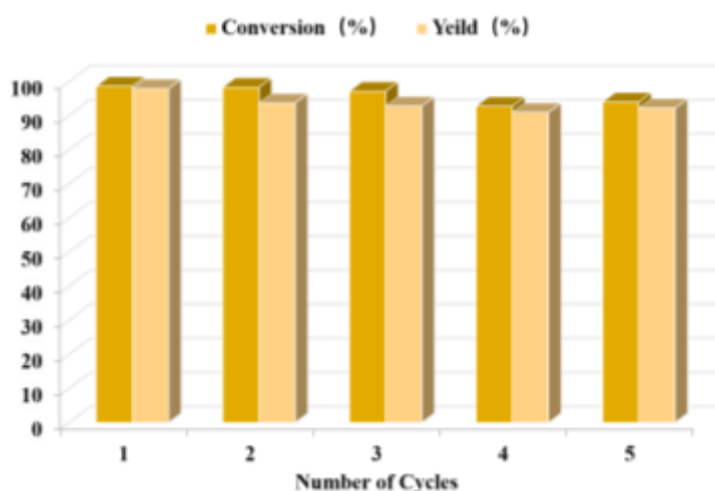


**Figure 6** The recyclability of  $WS_2$  nanosheets as catalyst.

The cyclic stability of the  $WS_2$  nanosheets as catalyst for benzylamine coupling was

investigated. The results of five cycle experiments were shown in Figure 6. High catalytic performance was maintained for every reaction cycle, and after five cycles, the conversion and yield of the coupling reaction still remained at 94.0% and 92.3%, indicating WS<sub>2</sub> nanosheets having high cyclic stability.

## Conclusion

Ultra-thin WS<sub>2</sub> nanosheets with 2H-phase were successfully synthesized by oil phase method, and assembled the products with flower-like morphology. TEM and HRTEM images revealed that there were many stripes on the surface of nanosheets, similar to texture of petal. The obtained WS<sub>2</sub> nanosheets had a strong absorption in the range of 200-800 nm, and exhibited strong fluorescence near 405 nm under excitation of 260 nm. Importantly, the WS<sub>2</sub> nanosheets possessed high photothermal co-catalytic activity for oxidative coupling of benzylamine and benzylamine homologues under natural light and air atmosphere at 60°C. Under typical catalytic conditions, the yield, conversion and selectivity of the coupling reactions reached as high as 97.91%, 98.61% and 99.29%, respectively. Besides, the WS<sub>2</sub> nanosheets had good catalytic stability and high catalytic activity still maintained after 5 cycles. The results show that the synthesized WS<sub>2</sub> nanosheets have a good catalytic application in the benzylamine coupling for imine, and are expected to replace the precious metal catalyst for the synthesis of imine in the future.

## Acknowledgements

The authors are thankful for the support rendered by the National Science Foundation of China (NSFC) (Grants 21641007), and Major Project of Education Department of Anhui Province (KJ2016SD63). We also thank the Key Laboratory of Environment Friendly Polymer Materials of Anhui Province.

**Keywords:** Tungsten disulfide nanosheets; Benzylamine; Photothermal co-catalysis; Coupling reaction; Imine

## References

- [1] X. Duan, C. Wang, A. Pan, R. Yu, X. Duan, *Chem. Soc. Rev.* **2015**, *44*, 8859.
- [2] L. Bian, W. Gao, J. Sun, M. Han, F. Li, Z. Gao, L. Shu, N. Han, Z. X. Yang, A. Song, Y. Qu, J. C. Ho, *ChemCatChem*. **2018**, *10*, 1571.
- [3] J. M. Song, J. Zhang, J. J. Ni, H. L. Niu, C. J. Mao, S. Y. Zhang, Y. H. Shen, *CrystEngComm*. **2014**, *16*, 2652.
- [4] K. T. Chen, S. T. Chang, *Vacuum*. **2017**, *140*, 172.
- [5] T. Georgiou, H. Yang, R. Jalil, J. Chapman, K. S. Novoselov, A. Mishchenko, *Dalton Trans.* **2014**, *43*, 10388.
- [6] H. R. Gutierrez, N. Perea-Lopez, A. L. Elias, A. Berkdemir, B. Wang, R. Lv, F. Lopez-Urias, V. H. Crespi, H. Terrones, M. Terrones, *Nano Lett.* **2013**, *13*, 3447.
- [7] M. Ratoi, V. B. Niste, J. Walker, J. Zekonyte, *Tribol. Lett.* **2013**, *52*, 81.
- [8] H. Feng, Z. Hu, X. Liu, *Chem. Commun.* **2015**, *51*, 10961.
- [9] Y. Zhu, H. Yi, Q. Hao, J. Liu, Y. Ke, Z. Wang, D. Fan, W. Zhang, *Appl. Surf. Sci.* **2019**, *485*, 101.
- [10] H. Yan, J. Li, D. Liu, X. Jing, D. Wang, L. Meng, *CrystEngComm*. **2018**, *20*, 2324.
- [11] B. Mahler, V. Hoepfner, K. Liao, G. A. Ozin, *J. Am. Chem. Soc.* **2014**, *136*, 14121.
- [12] H. Li, A. Li, Z. Peng, X. Fu, *Appl. Surf. Sci.* **2019**, *487*, 972.
- [13] F. Meng, W. Ma, C. Duan, X. Liu, Z. Chen, M. Wang, J. Gao, Z. Zhang, *Appl. Catal., B* **2019**, *252*, 187.
- [14] Q. Zhu, W. Chen, H. Cheng, Z. Lu, H. Pan, *ChemCatChem*. **2019**, *11*, 2667.
- [15] A. Rangaswamy, P. Sudarsanam, B. G. Rao B. M. Reddy, *Res. Chem. Intermed.* **2015**, *42*, 4937.
- [16] M. T. Schümperli, C. Hammond I. Hermans, *ACS Catalysis* **2012**, *2*, 1108.
- [17] L. L. Santos, P. Serna A. Corma, *Chemistry* **2009**, *15*, 8196.
- [18] A. Zanardi, J. A. Mata E. Peris, *Chemistry* **2010**, *16*, 13109.
- [19] A. Maggi R. Madsen, *Organometallics* **2011**, *31*, 451.
- [20] M. S. Kwon, S. Kim, S. Park, W. Bosco, R. K. Chidrala J. Park, *J. Organomet. Chem.* **2009**,

- 74, 2877.
- [21] J. Yang, C. Y. Mou, *Appl. Catal., B* **2018**, 231, 283.
- [22] S. Furukawa, A. Suga, T. Komatsu, *Chem. Commun.* **2014**, 50, 3277.
- [23] V. Panwar, S. L. Jain, *Mater. Sci. Eng. C Mater. Biol. Appl.* **2019**, 99, 191.
- [24] A. Griirane, A. Corma, H. Garcia, *J. Catal.* **2009**, 264, 138.
- [25] H. Guo, M. Kemell, A. Al-Hunaiti, S. Rautiainen, M. Leskelä, T. Repo, *Catal. Commun.* **2011**, 12, 1260.
- [26] D. Dissanayake, L. A. Achola, P. Kerns, D. Rathnayake, J. He, J. Macharia, S. L. Suib, *Appl. Catal., B* **2019**, 249, 32.
- [27] B. Q. Zhang, J. S. Chen, H. L. Niu, C. J. Mao, J. M. Song, *Nanoscale* 2018, 10(43), 20266.
- [28] M. Wang, H. Wu, C. Shen, S. Luo, D. Wang, L. He, C. Xia, G. Zhu, *ChemCatChem.* **2019**, 11, 1935.
- [29] Y. Fang, J. Pan, D. Zhang, D. Wang, H. T. Hirose, T. Terashima, S. Uji, Y. Yuan, W. Li, Z. Tian, J. Xue, Y. Ma, W. Zhao, Q. Xue, G. Mu, H. Zhang, F. Huang, *Adv Mater.* **2019**, 31,1901942.
- [30] P. G. Gassman, D. W. Macomber, S. M. Willging, *J. Am. Chem. Soc.* 1985, 107(8), 2380.
- [31] D. Barrera, Q. Wang, Y. J. Lee, L. Cheng, M. J. Kim, J. Kim, J. W. P. Hsu, *J. Mater. Chem. C* **2017**, 5, 2859.
- [32] S. Yeo, D. K. Nandi, R. Rahul, T. H. Kim, B. Shong, Y. Jang, J. S. Bae, J. W. Han, S. H. Kim, H. Kim, *Appl. Surf. Sci.* **2018**, 459, 596.
- [33] X. Zong, J. Han, G. Ma, H. Yan, G. Wu, C. Li, *J. Phys. Chem. C* **2011**, 115, 12202.
- [34] G. Costa, A. A. Assadi, S. Gharib-Abou Ghaida, A. Bouzaza, D. Wolbert, *Chem. Eng. J.* **2017**, 307, 785.
- [35] A. Berkdemir, H. R. Gutiérrez, A. R. Botello-Méndez, N. Perea-López, A. L. Elías, C. I. Chia, B. Wang, V. H. Crespi, F. López-Urías, J. C. Charlier, H. Terrones, M. Terrones, *Scientific Reports.* **2013**, 3, 1755.
- [36] F. Raza, J. H. Park, H. R. Lee, H. I. Kim, S. J. Jeon, J. H. Kim, *ACS Catalysis* **2016**, 6, 2754.
- [37] N. Zhang, X. Li, Y. Liu, R. Long, M. Li, S. Chen, Z. Qi, C. Wang, L. Song, J. Jiang, Y. Xiong, *Small* **2017**, 13, 1701354.
- [38] N. Zhang, X. Li, H. Ye, S. Chen, H. Ju, D. Liu, Y. Lin, W. Ye, C. Wang, Q. Xu, J. Zhu, L. Song, J. Jiang, Y. Xiong, *J. Am. Chem. Soc.* **2016**, 138, 8928.
- [39] Z. J. Wang, S. Ghasimi, K. Landfester, K. A. Zhang, *Adv. Mater.* **2015**, 27, 6265.

## Entry for the Table of Contents

Flower-like WS<sub>2</sub> composed of nanosheets like petals with several stripes on the surface were synthesized. As-synthesized WS<sub>2</sub> nanosheets showed excellent catalytic properties for oxidation coupling reaction of benzylamine under mild conditions without additional light and oxygen atmosphere. Further research showed that the

benzylamine oxidative coupling reaction was a photothermal co-catalytic process with thermal catalysis being dominant role and photocatalysis further improving the yield.

